

Atom Interferometry

Shohini Ghose

Department of Physics and Astronomy, University of New Mexico, Albuquerque, New Mexico

87131

(January 25, 2000)

Abstract

Atom interferometers are of interest because of their use as sensitive tools for the measurement of inertial forces, physical constants and various topological phases. In these devices, laser fields act as beam-splitters that split the atomic wave into two or more spatially separated states that accumulate different phases due to some external potential. When these states are recombined Ramsey fringes can be observed. The general theory of atom interferometers and, in particular of the Borde interferometer, is presented. Interferometry experiments for the measurement of gravity and rotational forces are described. Gravity measurements yield an uncertainty of $\delta g/g$ on the order of 10^{-9} , while the rotation sensors have a short term sensitivity of 10^{-8} rads/s. The phase shift induced by the dc Stark effect has also been measured using atom interferometers. Finally, experiments in which topological phases such as the Aharonov-Casher phase and Berry's phase have been measured are summarized and the accuracy of these measurements is analyzed.

PACS Numbers: 03.75.Dg, 03.65.Bz, 04.80.-y, 32.60.+i

Typeset using REVTeX

I. INTRODUCTION

Atom interferometry has fast become a powerful tool for the study of fundamental physical effects. The interference in these devices is caused by the superposition of atomic de Broglie waves. Atomic beams can be split and recombined in the same manner as optical beams by the use of laser pulses in order to create an interferometer [1]. The laser beams split the matter wave into two or more spatially separated arms that may get different phase shifts due to external potentials which, when the wave is recombined, results in Ramsey fringes. The primary use of atomic interferometers has been for the measurement of inertial forces such as acceleration due to gravity and rotations [2,3]. The large rest mass of atoms make these interferometers very sensitive to small phase shifts caused by such inertial forces. Another advantage of the use of atoms is their rich internal structure. Interaction of the atoms with electromagnetic fields can lead to potentials that cause a phase shift in the interference fringes. Such shifts can be used to make precision measurements of physical effects such as the dc Stark shift [4]. The non-dynamical or topological phase accumulated by a system due to the cyclic evolution of parameters in the system Hamiltonian can also be measured using atom interferometers. An example is the measurement of the Aharonov-Casher phase [5].

In Sec.II the general theory of atom interferometers and in particular the Ramsey method of separated fields that is commonly used in Bordé interferometers is presented. Section III consists of a description of typical atom interferometry experiments for the measurement of gravity gradients, rotations, the dc Stark shift and the Aharonov Casher phase. The accuracy and the factors limiting the precision of these measurements is discussed. Finally a summary and conclusion is included in Sec.IV.

II. THEORY

A. General Quantum Theory

Consider a Mach-Zender type of interferometer in which the atoms are split into two arms α and β by a beam splitter and later recombined in another beam splitter, after which they are detected in detector a or detector b depending on which path, α or β , the atom took (Fig.1). We assume that the wave function undergoes a $\pi/2$ phase shift upon reflection and a phase shift of $\phi_{1,2}$ upon transmission through the beam-splitters 1 and 2 respectively. The wave function of the i th atom after recombination is [6]

$$|\phi\rangle_i = \psi_a |1_a 0_b\rangle_i + \psi_b |0_a 1_b\rangle_i \quad (1)$$

where ψ_a and ψ_b are the amplitudes of the wave function at detectors a and b respectively.

$$\psi_a = \frac{e^{i\theta_a}}{2}(1 - e^{-i\phi_{\alpha\beta}}), \quad (2)$$

$$\psi_b = \frac{e^{i\theta_b}}{2}(1 + e^{-i\phi_{\alpha\beta}}). \quad (3)$$

$\theta_a = \pi/2 + kl_\alpha + \phi_2$ and $\theta_b = kl_\alpha + \phi_1 + \phi_2$ depend on the phases that are accumulated at the beam splitters and the mirrors, k is the wave vector and $\phi_{\alpha\beta} = k(l_\alpha - l_\beta)$ is the phase due to the path difference. The total state vector for N atoms is a product of the individual state vectors. The number operator for the number of atoms at detector a or b can be written as

$$N_\sigma = \sum_{i=1}^N a_{\sigma,i}^\dagger a_{\sigma,i} \quad (4)$$

where $\sigma = a, b$ and \hat{a} and \hat{a}^\dagger are the creation and annihilation operators obeying Bose or Fermi statistics. The atom statistics are important for high densities of atoms or if they are injected into the interferometer in a correlated manner. The expectation value of the number of particles in detector a is thus

$$\langle N_a \rangle = \sum_{i=1}^N \left| \frac{1 - e^{-i\phi_{\alpha\beta}}}{2} \right|^2 \langle 1_a, 0_b | n_{a,i} | 1_a, 0_b \rangle_i. \quad (5)$$

The number of atoms detected is thus modulated as the interferometer path difference is changed and one can observe interference fringes.

B. Ramsey's Separated Field Method

In order to implement atom interferometry, coherence-preserving atomic beam-splitters and mirrors are required. Recent advances in optics have made it possible to create such devices. In grating interferometers, coherent path separation is achieved by the diffraction of the atomic de Broglie waves by a solid amplitude grating or by a standing wave phase grating created by counter-propagating lasers [7,8]. Several elegant experiments using gratings have been performed [9,10]. The method of adiabatic transfer can also be used to create efficient mirrors [11,12].

In this article we will focus on the implementation of an atomic Mach-Zender interferometer by the Ramsey separated light field method [13,14]. For a two-level atom interacting with a laser field, the Hamiltonian can be written as

$$H = \hbar\omega_e |e\rangle \langle e| + \hbar\omega_g |g\rangle \langle g| - \vec{d} \cdot \vec{E} \quad (6)$$

where \vec{d} is the dipole moment and

$$\vec{E} = \vec{E}_0 \cos(\omega t + \phi). \quad (7)$$

Solving the Schroedinger equation for small detunings, the wave function amplitudes in the ground and excited state as a function of time are

$$c_e(t_0 + \tau) = e^{-i\delta\tau/2} \left(c_e(t_0) \cos \frac{\Omega_r \tau}{2} - i c_g(t_0) e^{-i(\delta t_0 + \phi)} \sin \frac{\Omega_r \tau}{2} \right), \quad (8)$$

$$c_g(t_0 + \tau) = e^{i\delta\tau/2} \left(-i c_e(t_0) e^{i(\delta t_0 + \phi)} \sin \frac{\Omega_r \tau}{2} + c_g(t_0) \cos \frac{\Omega_r \tau}{2} \right) \quad (9)$$

where Ω_r is the Rabi frequency and δ is the detuning. For the case of zero detuning we obtain the standard Rabi flopping

$$|c_e(\tau)|^2 = \frac{1}{2} [1 - \cos(\Omega_{eg}\tau)]. \quad (10)$$

Equation (2.8) can now be applied to the Ramsey $\pi/2 - \pi - \pi/2$ sequence of pulses with initial conditions $c_e(0) = 0, c_g(0) = 1$, a time T between each pulse and a duration $\tau/2$ of

the $\pi/2$ pulses . We assume that the Rabi frequency and detuning is the same for all the pulses but that the phase, ϕ_i of each pulse may vary. The occupation probability of the excited state can be calculated to be

$$|c_e(2\tau + T)|^2 = \frac{1}{2}[1 - \cos(\Delta\phi - \delta T)], \quad (11)$$

where

$$\Delta\phi = \phi_1 - 2\phi_2 + \phi_3 \quad (12)$$

is the phase difference between the three pulses. The probability of finding the atom in the excited state will yield Ramsey fringes as a function of the phase $\Delta\phi$ of the lasers or the detuning δ .

C. The Atomic Mach-Zender Interferometer

The Ramsey method presented in the previous section constitutes an interferometer in the Hilbert space of ground and excited state. However the external degrees of freedom have been neglected. In general, the absorption of a photon by an atom is accompanied by a recoil of $\hbar k$ by the excited atom. Emission of a photon causes an opposite recoil. The difference between the photon energy $\hbar\omega_0$ and the internal atomic energy $\hbar\omega_L$ must be the extra kinetic energy of the recoil. This energy conservation condition can be written as

$$\frac{\mathbf{p}^2}{2m} + \hbar\omega_L = \frac{(\mathbf{p} + \hbar\mathbf{k})^2}{2m} + \hbar\omega_0. \quad (13)$$

This equation can be solved for the atomic wave vector \mathbf{k} . The complete basis of internal and external states is now $|g, \mathbf{p}\rangle$ and $|e, \mathbf{p} + \hbar\mathbf{k}\rangle$ and the wave can be written as

$$|\psi(t)\rangle = c_{e, \mathbf{p} + \hbar\mathbf{k}}(t) |e, \mathbf{p} + \hbar\mathbf{k}\rangle e^{-i\left(\omega_e + \frac{|\mathbf{p} + \hbar\mathbf{k}|^2}{2m\hbar}\right)t} + c_{g, \mathbf{p}}(t) |g, \mathbf{p}\rangle e^{-i\left(\omega_g + \frac{|\mathbf{p}|^2}{2m\hbar}\right)t} \quad (14)$$

with a modified detuning of

$$\delta = \omega - \left(\omega_{eg} + \frac{\mathbf{p} \cdot \mathbf{k}}{m} + \frac{|\mathbf{p}|^2}{2m\hbar} \right). \quad (15)$$

In the $\pi/2 - \pi - \pi/2$ pulse sequence of Fig.2(a), the $\pi/2$ pulses create an equal superposition of ground and excited state. The excited state wave function receives a recoil of $\hbar\mathbf{k}$ along the direction of the laser beam while the ground state wave function continues to propagate in the initial direction of motion. Therefore the excited state spatially separates from the ground state. The $\pi/2$ pulses thus act as 50/50 beam splitters.

The π pulse flips ground and internal states so that the excited state gets a negative recoil of $\hbar\mathbf{k}$ as it goes to the ground state while the ground state gains a momentum of $\hbar\mathbf{k}$ as it changes to the excited state. The π pulse thus acts like a mirror for the atomic wave function. The entire $\pi/2 - \pi - \pi/2$ sequence is therefore identical to a Mach-Zender interferometer as shown in Fig. 2.

In order to increase the spatial separation of the two arms one can use sequences consisting of more pulses. The Ramsey-Bordé sequence consists of two pairs of counter-propagating $\pi/2$ pulses (Fig.2(b)). A larger enclosed area can increase the sensitivity of the interferometer for measuring inertial forces [15,2,16]. However the use of more pulses also increases the sensitivity of the interferometer to noise in the intensity and phase of the lasers. Furthermore, the repeated splitting of the wave function by additional $\pi/2$ pulses causes the final detected signal intensity to decrease.

III. EXPERIMENTS

A. Measurement of Inertial Forces

The Ramsey sequence yields fringes as a function of the relative phase $\Delta\phi$ of the laser fields (Eq.2.11). In the presence of inertial forces the two arms of the interferometer might accumulate additional phases that cause a net shift of the fringe pattern. For atoms falling under the force of gravity the frequency and phase of the lasers is Doppler shifted so that the phase of laser i at time t is

$$\phi_i(t) = \omega_i t - \vec{k} \cdot \vec{g} t^2 + \phi_i^0. \quad (16)$$

In the $\pi/2 - \pi - \pi/2$ pulse sequence, if the frequency of the lasers is changed in a phase continuous way, such that the laser is always resonant with the $|g, \mathbf{p}\rangle$ to $|e, \mathbf{p} + \hbar\mathbf{k}\rangle$ transition, then the $\omega_i t$ terms drop out of the net phase $\Delta\phi$ of equation (2.11) [15]. The only extra phase shift is the kgT^2 term.

Recent measurements of this phase shift have resulted in a value of g with an absolute uncertainty of $\delta g/g = 3 \times 10^{-9}$ [15]. The internal states used in the experiment are two magnetic field insensitive hyperfine ground states of cesium. Two photon Raman transitions which cause twice the momentum recoil are induced by pairs of counter-propagating lasers. Laser cooled cesium atoms are launched at $1.5\mu K$ and are subjected to preparation, Raman and detection pulses (Fig.3). Since the Raman beams travel the same path before entering the system, any frequency shift caused by external vibrations is the same for both beams. Typical pulse spacings are $T=160ms$, and for one minute of integration time, one can determine g to a precision of 3×10^{-9} (Fig.4). The main noise sources are mechanical vibrations that change the laser frequency and phase noise of the source. Further improvements can be made by eliminating systematic errors such as the Coriolis effect. Another setup that better cancels out vibration errors is discussed in reference [3].

Atom interferometers are also used for rotation sensing [2,16]. Consider an interferometer with a circular path of radius R rotating at Ω rads/s. The velocities of the co-rotating and counter-rotating arms relative to the rotating frame are thus shifted by $\pm 2\Omega R$. The two beams travel slightly different path lengths before recombination due to the rotation. One can show that the net phase shift due to the path length difference is

$$\Delta\phi = \frac{2m}{\hbar}A\Omega, \quad (17)$$

where A is the area enclosed. The proportionality of the phase shift to the area can be shown to hold true for any shape of area enclosed. This shift is called the Sagnac phase shift.

Experiments similar to the gravity measurement experiments in which two-photon Raman transitions are driven between cesium hyperfine states have also been performed to make

precision rotation measurements [2]. The experimental set-up is shown in Fig.5. Preparation involves optically pumping the atoms into a magnetically insensitive hyperfine state. After the usual $\pi/2 - \pi - \pi/2$ Raman pulse sequence, the ground state F=3 to F=4 transition is detected by resonance fluorescence. The fringes are offset from zero due to the rotation rate of the earth that has to be compensated for. There is some loss of contrast due to the averaging of the phase shift over the longitudinal velocity distribution. Again the main sources of errors are vibration as well as alignment of the Raman beams. An advantage of the Raman beam method is that the line width can be adjusted to address large velocity spreads.

The sensitivity of the measurement is 2×10^{-8} rads/s. This sensitivity can be increased by using multiple pulse sequences to increase the enclosed area. Also if a counter-propagating atomic beam is introduced and the difference in the phase shifts of the two beams is taken, many systematic errors cancel out. It has also been shown that by adding an additional potential V_o the sensitivity to rotations can be increased [17].

B. Measurement of the dc Stark shift

The internal structure of an atom can be probed by causing the atom to interact with an electromagnetic field. For example, when an electric field, E is applied to one arm of a Ramsey interferometer, the dipole interaction leads to an external potential in terms of the atomic polarizability α

$$V(x) = -\frac{1}{2}\alpha E(x)^2. \quad (18)$$

The external potential affects the motion of the wave packet in this arm of the interferometer which leads to a path difference between the two arms,

$$\Delta x \propto \int V(x) dx. \quad (19)$$

The path difference results in an extra phase shift of $k\Delta x$. The dc Stark shift of the Mg intercombination line has been measured using a Bordé interferometer consisting of a beam

of Mg atoms passing through two pairs of counter-propagating $\pi/2$ laser pulses [4]. When the frequency of the lasers is scanned interference fringes are obtained (Eq.2.11). An electric field is then applied by placing a capacitor between the two pairs of laser beams. An additional magnetic field is applied in order to select the $m_x = 0$ state (Fig.6). Since the separated atomic wave packets are in different internal states, the two arms experience different Stark shifts. The electric field can therefore extend over both arms. The resulting potential difference leads to a shift of the fringes as the frequency is scanned, relative to the initial scan without the electric field. The population in the exit port is measured by counting the fluorescence of the excited state with a photo-multiplier. The frequency shift as a function of voltage across the capacitor can be measured to obtain a value for the difference in polarizabilities of the $3s^2(^1S_0)$ and the $3s3p(^3P_1)$ states of $8.0 \pm 1.0 \text{ kHz (kV/cm)}^{-2}$. This is in reasonably good agreement with the theoretically calculated difference of $6.3 \pm 2.0 \text{ kHz (kV/cm)}^{-2}$. The main sources of error are due to uncertainties in the statistical fitting of the data and an incomplete knowledge of the electric field distribution.

The dc Stark shift has also been measured using calcium atoms in a similar Bordé interferometer set-up [18]. The measurements of the dc and ac Stark shift are important since these effects must be corrected for when using such atoms as optical frequency standards.

C. Measurement of Topological phases

A quantum system that evolves cyclically in the parameter space of the Hamiltonian can accumulate a time-independent geometric (Berry's) phase in addition to the usual dynamical phase as first shown by Berry [19]. Geometric phases can be topological phases that do not depend on the trajectory of the particle. An example of a topological phase is the Aharonov-Casher phase shift acquired by a magnetic dipole moment that follows a closed path around a charged wire [20,21],

$$\Delta\phi_{AC} = \frac{1}{\hbar c^2} \oint \vec{\mu} \times \vec{E} \cdot d\vec{r}. \quad (20)$$

The Aharonov-Casher phase can be measured via several different techniques [5,22,23]. Initial experiments were performed by letting the two arms of an atomic beam with magnetic moment μ encircle a line charge and then recombining the beams to measure the interference. An equivalent set-up is to have the two arms of the atomic beam have opposite magnetic moments and let them pass through the same electric field [5]. In this case since the two arms will accumulate opposite phases, there is no need to spatially separate them. The interference occurs in the parameter space of magnetic ‘up’ and ‘down’ states. Such an experiment was performed using thallium fluoride molecules prepared in a coherent superposition of opposite spin states using an rf magnetic field (Fig.7). The particles then travel a length of $l=2.05\text{m}$ in a strong (10-30V/cm) external electric field. A second rf magnetic field acts as the second beam splitter after which the internal state population is measured. Since the spins tend to align along the direction of the electric field, a magnetic field is used to give the spins a component perpendicular to the field. This component gives the $\vec{\mu} \times \vec{E}$ phase shift. The phase shift measurement had an accuracy greater than 99% when compared to the theoretical value. The velocity independence and the proportionality of the phase shift to the electric was also demonstrated.

Another major type of geometric phase occurs in the adiabatic evolution of a spin in a magnetic field or, equivalently, a two-level atom in an electromagnetic field. Recent experiments to measure the Berry’s phase of atoms in an optical lattice have been performed [24].

IV. CONCLUSIONS

Even though the field of atom interferometry is relatively young, a wide range of experiments have already been performed. These experiments have shown that atom interferometers are versatile devices and can be used to make highly sensitive measurements. The measurements of gravity and rotation are of importance for geophysics and navigation. The ability to measure phases due to physical effects such as the Stark shift as well as geometric

phases is necessary if atoms are to be used as frequency standards. In precision measurements of frequency standards, a standard tool used is the Ramsey method of two separated light fields. The Bordé scheme of atom interferometry might prove to be a more precise technique than the standard Ramsey method and is capable of relative precision and accuracy in the range of 10^{-15} . Another rich area of research is the atom-interferometric study of Bose-Einstein condensation [25]. The future holds many applications of atom interferometry to make a wide variety of precision measurements.

REFERENCES

- [1] *Atom Interferometry*, edited by P. Berman (Academic Press, San Diego, CA 92101-4495, USA, 1997).
- [2] T. L. Gustavson, P. Bouyer, and M. A. Kasevich, *Phys. Rev. Lett.* **78**, 2046 (1997).
- [3] M. J. Snadden, J. M. McGuirk, P. Bouyer, K. G. Haritos, and M. A. Kasevich, *Phys. Rev. Lett.* **81**, 971 (1998).
- [4] V. Reiger, K. Sengstock, U. Sterr, J. H. Müller, and W. Ertmer, *Opt. Comm.* **99**, 172 (1993).
- [5] K. Sangster, E. A. Hinds, S. Barnett, and E. Riis, *Phys. Rev. Lett.* **71**, 3641 (1993).
- [6] M. O. Scully and M. S. Zubairy, *Quantum Optics* (Cambridge University Press, Cambridge, CB2 2RU, UK, 1997).
- [7] S. Altshuler, L. M. Frantz, and R. Braunstein, *Phys. Rev. Lett.* **17**, 231 (1966).
- [8] V. Chebotayev, B. Y. Dubetsky, A. P. Kasantsev, and V. P. Yakovlev, *J. Opt. Soc. Am. B* **2**, 1791 (1985).
- [9] P. E. Moskowitz, P. L. Gould, and D. E. Pritchard, *J. Opt. Soc. Am. B* **2**, 1784 (1985).
- [10] P. J. Martin, B. G. Oldaker, A. H. Miklich, and D. E. Pritchard, *Phys. Rev. Lett.* **60**, 515 (1988).
- [11] J. R. Kuklinski, U. Gaubatz, F. T. Hioe, and K. Bergmann, *Phys. Rev. A* **40**, 6741 (1989).
- [12] P. Marte, P. Zoller, and J. L. Hall, *Phys. Rev. A* **44**, R4118 (1990).
- [13] N. F. Ramsey, *Phys. Rev.* **78**, 695 (1950).
- [14] C. J. Bordé, *Phys. Lett.* **140**, 10 (1989).
- [15] A. Peters, K. Y. Chung, and S. Chu, *Nature* **400**, 849 (1999).

- [16] A. Lenef, T. Hammond, E. Smith, M. Chapman, R. Rubenstein, and D. Pritchard, Phys. Rev. Lett. **78**, 760 (1997).
- [17] M. Özcan, J. Appl. Phys. **83**, 6185 (1998).
- [18] A. Morinaga, M. Nakamura, T. Kuroki, and N. Ito, Phys. Rev. A **54**, R21 (1996).
- [19] M. V. Berry, Proc. R. Soc. London, Ser. A **392**, 54 (1984).
- [20] Y. Aharonov and A. Casher, Phys. Rev. Lett **53**, 319 (1984).
- [21] J. Anandan, Phys. Rev. Lett. **48**, 1660 (1982).
- [22] A. Görlitz, B. Schuh, and A. Weis, Phys. Rev. A **51**, R4305 (1995).
- [23] J. H. Müller, D. Bettermann, V. Reiger, K. Sengstock, U. Sterr, and W. Ertmer, Appl. Phys. B **60**, 199 (1995).
- [24] C. L. Webb, R. M. Godun, G. S. Summy, M. K. Oberthaler, P. D. Featonby, C. J. Foot, and K. Burnett, Phys. Rev. A **60**, R1783 (1999).
- [25] T. Altenmüller, R. Müller, and A. Schenzle, Phys. Rev. A **56**, 2959 (1997).

FIGURES

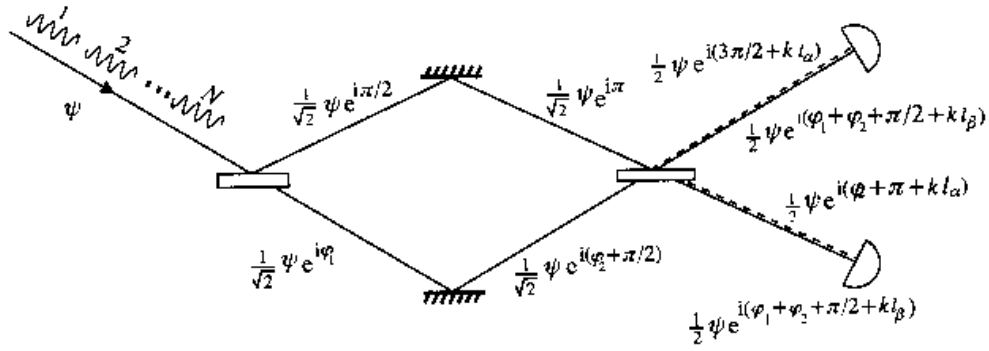


FIG. 1. Schematic for an atom interferometer[M. O. Scully and M. S. Zubairy, *Quantum Optics* (Cambridge University Press, Cambridge, CB2 2RU, UK, 1997)]. The wave function accumulates different phases due to the mirrors and beam splitters in the two different arms.

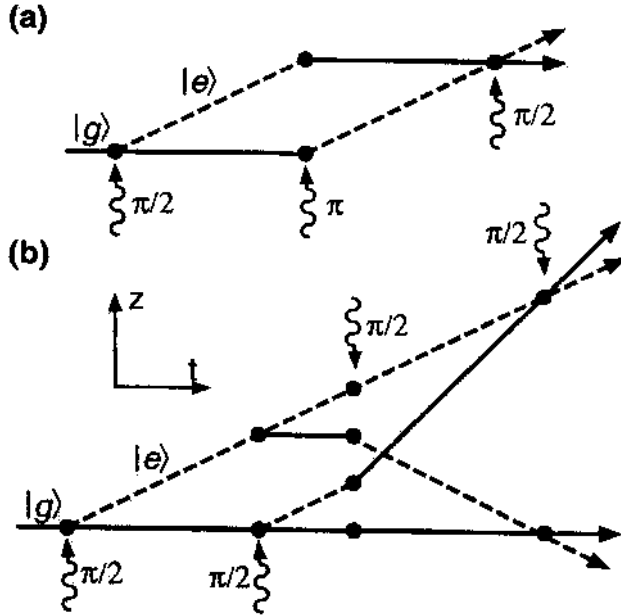


FIG. 2. Recoil diagrams for (a) the $\pi/2 - \pi - \pi/2$ geometry and (b) the Ramsey-Bordé sequence[*Atom Interferometry* , edited by P. Berman (Academic Press, San Diego, CA 92101-4495, USA, 1997)].

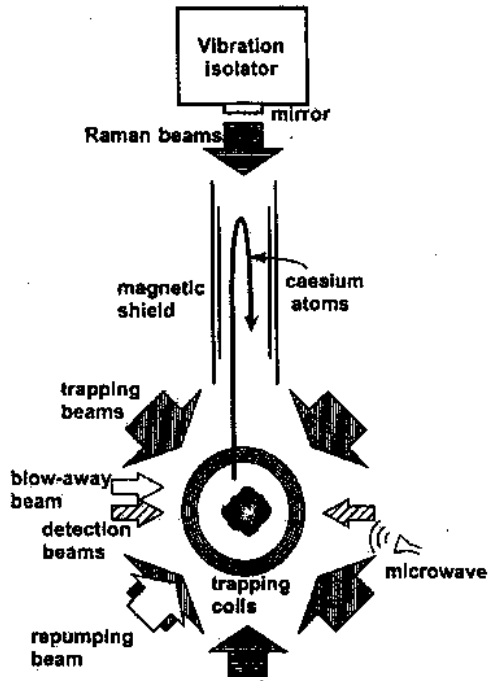


FIG. 3. Measurement of g using raman transitions to drive the $\pi/2 - \pi - \pi/2$ sequence [A. Peters, K. Y. Chung, and S. Chu, *Nature* **400**, 849 (1999)].

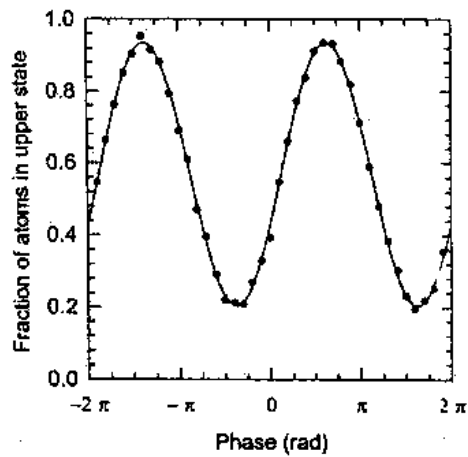


FIG. 4. Interferometric fringes for the g measurement [A. Peters, K. Y. Chung, and S. Chu, *Nature* **400**, 849 (1999)]. One full fringe corresponds to $2 \times 10^6 g$.

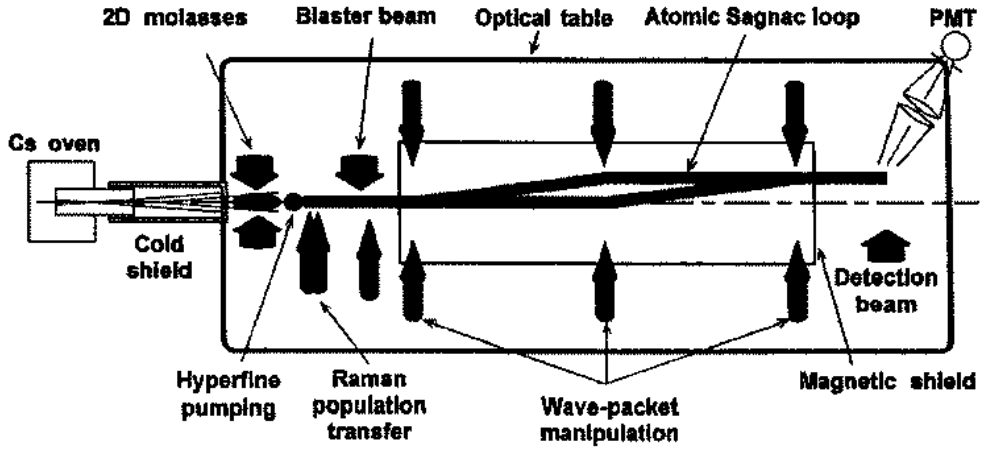


FIG. 5. Apparatus for rotation measurements also using two-photon stimulated raman transitions to drive the $\pi/2 - \pi - \pi/2$ sequence [T. L. Gustavson, P. Bouyer, and M. A. Kasevich, Phys. Rev. Lett. **78**, 2046 (1997)].

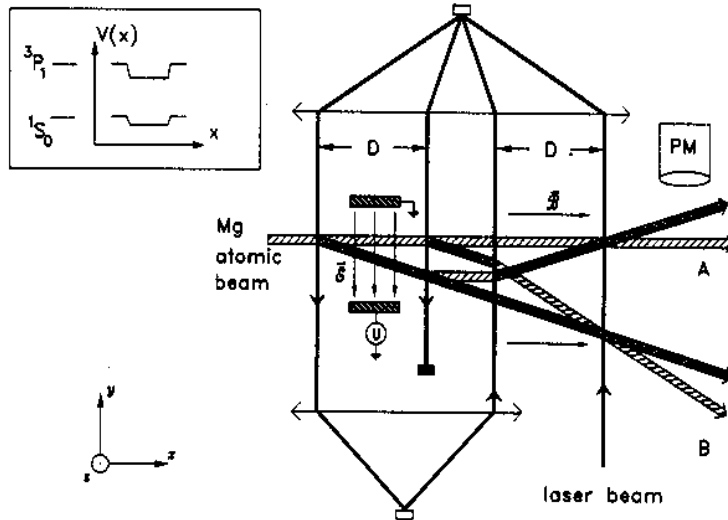


FIG. 6. Measurement of the dc Stark shift using Mg atoms [V. Reiger, K. Sengstock, U. Sterr, J. H. Müller, and W. Ertmer, Opt. Comm. **99**, 172 (1993)]. The Stark effect leads to a potential $V(x)$ between the capacitor plates.

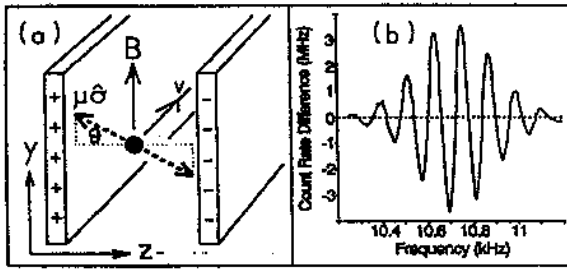


FIG. 7. Experimental configuration for measuring the AC phase [K. Sangster, E. A. Hinds, S. Barnett, and E. Riis, *Phys. Rev. Lett.* **71**, 3641 (1993)]. An rf magnetic field is used as the 50/50 beamsplitters. Spatial separation of the atomic beam is not necessary since the two arms have opposite magnetic moments and get different phases.